Thermal Inelastic Scattering of Cold Neutrons in Polycrystalline Graphite. II

P. G. KHUBCHANDANI, L. S. KOTHARI, AND K. S. SINGWI
Atomic Energy Establishment, Trombay, Bombay, India
(Received October 23, 1957)

Inelastic scattering cross section of cold neutrons in polycrystalline graphite is calculated without using the incoherent approximation. The present calculations, though they are an improvement upon those reported in an earlier paper, are still unable to explain satisfactorily the observed variation of cross section with neutron wavelength. Calculations of some typical scattering surfaces in graphite are also given, revealing some interesting features.

I. INTRODUCTION

IN an earlier paper[1] we reported the calculations, using the incoherent approximation, of the inelastic scattering cross section of cold neutrons in graphite. Though the variation of the cross section with temperature for 10 A neutrons was in fairly good agreement with the experimental results, the wavelength dependence of the cross section was in disagreement with the observed values. This prompted us to recalculate the scattering cross section without making use of the incoherent approximation. The results of these calculations are briefly presented and discussed in the next two sections. The last section deals with some typical scattering surfaces in graphite.

II. COHERENT ONE-PHONON CROSS SECTION

The coherent one-phonon absorption cross section is obtained by multiplying the term proportional to S in Eq. (24) of Kothari and Singwi[2] by $k_2/16\pi^2Nk_1$ and putting $l=1$. Carrying out the summation over the lattice points σ, we obtain after some modification

$$d\sigma_1=\frac{2\pi^2Sk_2F_\tau^2}{NBMk_1n^2}\left|\sum_s(\mathbf{k}_1-\mathbf{k}_2\cdot\boldsymbol{\varepsilon}_s)^2\right|\xi^{-1}(e^{\xi/T}-1)^{-1}\times\exp\left\{-\frac{1}{MN}(\mathbf{k}_1-\mathbf{k}_2\cdot\boldsymbol{\varepsilon}_s)^2\sum\xi^{-1}\coth\frac{\xi}{2T}\right\}\times\delta(\mathbf{k}_1-\mathbf{k}_2+\mathbf{f}-2\pi\boldsymbol{\tau}),\quad(1)$$

where F_τ is the form factor corresponding to the reciprocal lattice vector $\boldsymbol{\tau}$, n is the number of carbon atoms per cell, B is the volume per carbon atom, and $\mathbf{f}$ is the wave vector of a phonon of energy ξ. As in I, all quantities are expressed in dimensionless units and have the same significance.

Let us consider the contribution to the scattering cross section arising from vibrations of the atoms in the basal plane. Integrating over the various directions of $\mathbf{k}_2$ and averaging over the directions of $\mathbf{k}_1$, we obtain[3]

$$\sigma_1^{(xy)}(\xi)=\frac{\pi^2SF_\tau^2}{NBMk_1^2n^2}\xi^{-1}(e^{\xi/T}-1)^{-1}\frac{(2\pi\boldsymbol{\tau}-\mathbf{f})_{xy}^2}{|2\pi\boldsymbol{\tau}-\mathbf{f}|}\times\exp\left[-\frac{2F_1}{M}(2\pi\boldsymbol{\tau}-\mathbf{f})_{xy}^2\right].\quad(2)$$

This has now to be summed over all allowed values of $\mathbf{f}$. This summation may be replaced by an integration without introducing much error,

$$\sum_f\rightarrow\frac{2N(\varphi_+-\varphi_-)}{\pi\Theta^2}\int\xi d\xi,\quad(3)$$

since $\mathbf{f}$ *lies only in the basal plane*, and φ_+, φ_- are determined from the momentum conservation condition

$$|k_1-k_2|\leqslant|2\pi\boldsymbol{\tau}-\mathbf{f}|\leqslant k_1+k_2,\quad(4)$$

where

$$(2\pi\boldsymbol{\tau}-\mathbf{f})^2=(2\pi\tau)^2+f^2-4\pi f\tau_{xy}\cos\varphi,\quad(5)$$

φ being the angle between $\mathbf{f}$ and $\boldsymbol{\tau}_{xy}$. From (4) and (5) it follows that the upper and lower limits φ_+ and φ_- of φ are, respectively, given by

$$\cos\varphi_\pm=\frac{(2\pi\tau)^2+f^2-(k_1\pm k_2)^2}{4\pi f\tau_{xy}}$$

if $-1<$right-hand side<1, (6)

$=1$ if right-hand side>1,

$=-1$ if right-hand side<-1.

If $\tau_{xy}=0$ for some $\boldsymbol{\tau}$, then

$$\varphi_+-\varphi_-=\pi,\quad\text{if}\quad|k_1-k_2|\leqslant\{(2\pi\tau)_z^2+f^2\}^{\frac{1}{2}}\leqslant k_1+k_2,$$

and is zero otherwise.

Making use of (3) and summing over the reciprocal lattice vectors, we have for the cross section

$$\sigma_1^{(xy)}=\frac{2\pi S}{MBk_1^2n^2\Theta^2}\int_\epsilon^\Theta\sum_\tau M_\tau F_\tau^2(\varphi_+-\varphi_-)\frac{(2\pi\tau)_{xy}^2}{2\pi\tau}\times\exp\left[-\frac{2F_1}{M}(2\pi\tau)_{xy}^2\right](e^{\xi/T}-1)^{-1}d\xi,\quad(7)$$

where M_τ is the multiplicity of τ. We have here neglected f in comparison to $2\pi\tau$.

[1] L. S. Kothari and K. S. Singwi, Phys. Rev. **106**, 230 (1957), hereafter referred to as I.
[2] L. S. Kothari and K. S. Singwi, Proc. Roy. Soc. (London) **A231**, 293 (1955). The notation used in the present paper is the same as that used in I.
[3] R. Weinstock, Phys. Rev. **65**, 1 (1944).

Similarly the contribution to the cross section arising from vibrations perpendicular to the basal plane, is

$$\sigma_1^{(z)}=\frac{2\pi S}{MBk_1^2n^2}\int_\epsilon^1 \sum_\tau M_\tau F_\tau^2(\varphi_+-\varphi_-)\frac{(2\pi\tau)_z^2}{2\pi\tau} \times\exp[-(2F_2/M)(2\pi\tau)_z^2](e^{\xi/T}-1)^{-1}d\xi. \quad (8)$$

III. DISCUSSION

Graphite is a hexagonal lattice with $a=2.461$ A and $c=6.709$ A and contains four atoms ($n=4$) per unit cell placed at the positions

$$(0\ 0\ 0),\quad (0\ 0\ \tfrac{1}{2}),\quad (\tfrac{1}{3}\ \tfrac{2}{3}\ 0),\quad (\tfrac{2}{3}\ \tfrac{1}{3}\ \tfrac{1}{2}).$$

The volume of the cell per carbon atom is $B=8.979\times10^{-24}$ cm^3. The square of the form factor, defined as

$$F_\tau=|\sum \exp[2\pi i(hx+ky+lz)]|^2,$$

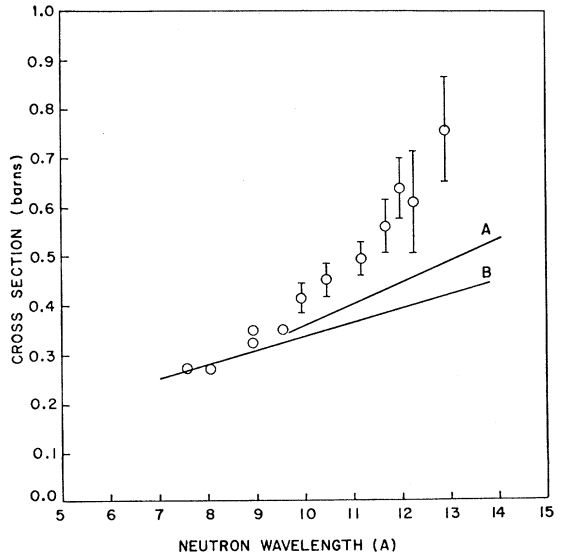

FIG. 1. Total cross section plotted against neutron wavelength for graphite temperature of 300°K. Curve A, present calculations. Curve B, calculations on the incoherent approximation. Φ, experimental points. $\sigma_a=0.0025$ barn/A.

reduces, in the present case, to

$$F_\tau^2=6+4\cos[\tfrac{2}{3}\pi(h+2k)]+4\cos[\tfrac{2}{3}\pi(2h+k)] +2\cos[\tfrac{2}{3}\pi(h-k)]\quad\text{for } l \text{ even} \quad (9)$$
$$=4\sin^2[\tfrac{1}{3}\pi(h-k)]\quad\text{for } l \text{ odd}.$$

From (7) and (8) and using these and other constants as given in I, we have calculated both $\sigma_1^{(xy)}$ and $\sigma_1^{(z)}$. The results obtained for the variation of the cross section with wavelength are shown in Fig. 1 as curve A. Curve B gives the corresponding results when the incoherent approximation is used.

The correction to the incoherent approximation varies with wavelength and is as much as 23% for $\lambda=14$ A. The present calculations have improved upon the earlier ones, but they are still not in good agreement with observations. As discussed in I, at least a part of the discrepancy may be due to small-angle scattering.

TABLE I. Total one-phonon scattering cross section in barns for neutrons of 10 A wavelength, for graphite at various temperatures.

T°K	σ (in barns) earlier value	σ (in barns) present value
100	0.03	0.04
200	0.14	0.16
300	0.31	0.34
500	0.75	0.79
700	1.33	1.27
900	1.98	1.71

In a recent paper Egelstaff[4] gives a value of about 0.6 barn for the inelastic scattering cross section of 8 A neutrons. This is almost twice the value obtained by Palevsky, quoted in I. Egelstaff points out that the cross-section measurements in graphite are always vitiated by a large small-angle scattering (about 4 barns at $\lambda=15$ A) and by the preferential orientation of the graphite grains in the sample. In view of this, it may be difficult to make an exact comparison of theory and experiment, particularly insofar as the variation of cross section with wavelength is concerned.

The temperature dependence of the cross section is not appreciably altered from the earlier calculations, as can be seen from Table I.

IV. SCATTERING SURFACES

Because of the layer structure of graphite, the wave vector of the phonons essentially lies in the basal plane. This leads to some peculiarities in the scattering surfaces (locus of $\mathbf{k}_2$ which satisfies both the energy and momentum conservation conditions, for given values of $\mathbf{k}_1$ and $\boldsymbol{\tau}$), when compared with similar surfaces for more or less isotropic lattices. Planes of the type $hk0$, i.e., those for which the reciprocal lattice vector lies in the basal plane, would show no peculiarities and in the xy projection (Fig. 2) one would

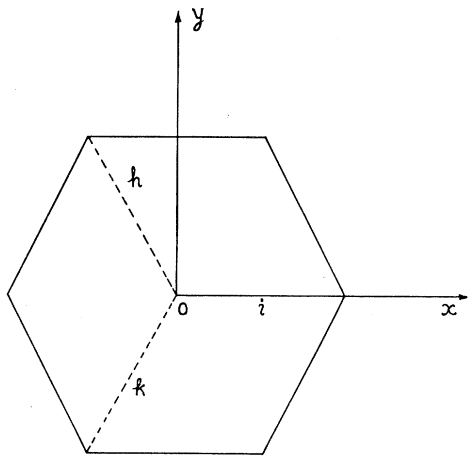

FIG. 2. Set of axes for graphite. The z axis is parallel to the c axis (perpendicular to the plane of the diagram).

[4] P. A. Egelstaff, J. Nuclear Energy **5**, 203 (1957).

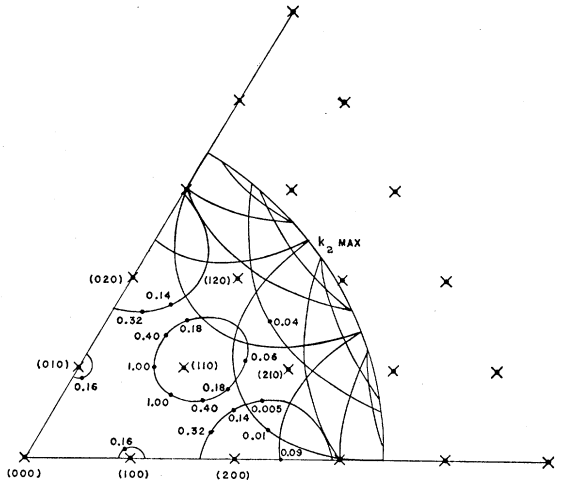

FIG. 3. Scattering surfaces for $k_1=0$ and the $hk0$ planes. The numbers in parentheses indicate coordinates of the reciprocal lattice points marked by a cross. Relative values of the scattering cross section at a few points on the scattering surfaces are also indicated. The maximum value of k_2 is $\Theta^{\frac{1}{2}}$.

obtain a continuous curve for the allowed values of k_2 for any given k_1. Since $\tau_z=0$ for these planes, it follows from (8) that, under the approximations made, $\sigma_1^{(z)}$ would be zero and only the xy modes of vibration will contribute to the scattering. An example of the scattering surfaces for $k_1=0$ and for the $hk0$ planes is given in Fig. 3. Since it is the xy modes that scatter, $k_{2,\max}=\Theta^{\frac{1}{2}}$. The relative values of the scattering cross section at a few points on the scattering curves are also indicated in the same figure.

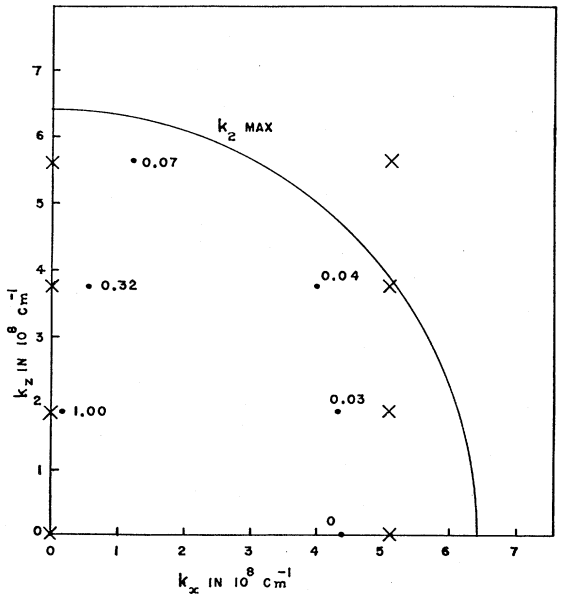

FIG. 4. Scattering surfaces (here points) for $k_1=0$ and the hhl planes. The crosses indicate reciprocal lattice points in the xz plane. The vectors joining the origin to the various solid circles are the only allowed directions of scattering. The numbers alongside indicate relative scattering cross sections.

In Fig. 4 are plotted scattering surfaces for $k_1=0$ and for the hhl planes, i.e., planes whose reciprocal lattice vector lies in the xz plane. Since the component of $\mathbf{f}$ along the z axis is zero, these surfaces just reduce to a maximum of two points. Contribution to the scattering comes mainly from the z modes, and the relative cross sections along the allowed directions are indicated by numbers put alongside the points. Maximum scattering comes from the 002 plane. Long-wavelength neutrons scattered from hhl planes of a single crystal of graphite will be observed in the xz plane only along certain given directions and the energy distribution of these neutrons would also show a sharp peak. Also very cold neutrons scattered from these planes will be observed mainly along the z axis (c axis of graphite).

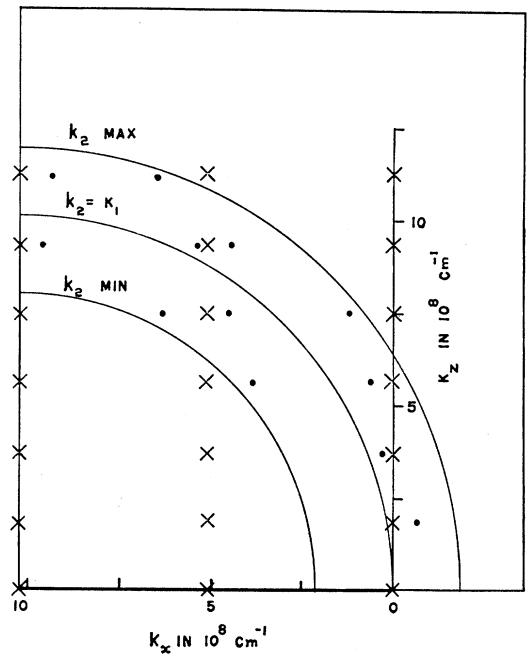

FIG. 5. Scattering surfaces (here points) for $k_1=10.212\times10^8$ cm^{-1} and the hhl planes. The crosses indicate reciprocal lattice points in the xz plane. The vectors joining the origin to the various solid circles are the only allowed directions of scattering.

Scattering "points" for the same set of planes but for a finite k_1, $k_1=10.212\times10^8$ cm^{-1}, are plotted in Fig. 5. Allowed values of k_2 lie within segments of radii $k_{2,\max}=10.06\times10^8$ cm^{-1} and $k_{2,\min}=7.94\times10^8$ cm^{-1}.

It may be noted that whereas the scattering from the $hk0$ planes is essentially due to the xy modes, the scattering from the hhl planes is due to the z modes. This could thus provide a means of studying the two modes independently. For example, because of the much smaller value of Θ_z as compared to the value of Θ_{xy}, the temperature dependence of the scattering from the hhl planes would be far more pronounced. It would be interesting to do experiments with a single crystal of graphite and check some of the above results.